crystals

MDPI

Article

Crucial Role of Oxygen Vacancies in Scintillation and Optical Properties of Undoped and Al-Doped β-Ga_2O_3 Single Crystals

Ruifeng Tian [1,2], Mingyan Pan [1,*], Qinglin Sai [1], Lu Zhang [1,2], Hongji Qi [1,*] and Hany Fathy Mohamed [1,3]

[1] Key Laboratory of Materials for High Power Laser, Shanghai Institute of Optics and Fine Mechanics, Chinese Academy of Sciences, Shanghai 201800, China; ruifengtian@siom.ac.cn (R.T.); saiql@siom.ac.cn (Q.S.); zhanglu@siom.ac.cn (L.Z.); h.fathy@science.sohag.edu.eg (H.F.M.)
[2] Center of Materials Science and Optoelectronics Engineering, University of Chinese Academy of Sciences, Beijing 100049, China
[3] Physics Department, Faculty of Science, Sohag University, Sohag 82524, Egypt
* Correspondence: pmy@siom.ac.cn (M.P.); qhj@siom.ac.cn (H.Q.)

Abstract: In this paper, the effects of oxygen vacancy and gallium vacancy on the optical and scintillation properties of undoped β-Ga_2O_3 crystal and 2.5 mol % Al doped gallium oxide were investigated. For the undoped β-Ga_2O_3, the transmittance is improved after annealing in oxygen or nitrogen atmosphere. After the introduction of Al element, the absorption cutoff appears slightly blue shift, and the band gap increases. For the undoped as-grown β-Ga_2O_3 single crystals, the decay time consists of a fast component (τ_1) of the order of nanoseconds, and two slow components (τ_2, τ_3) of tens to hundreds of nanoseconds. The contribution of the fast decay time component in the decay times is 2.78%. While for Al-doped β-Ga_2O_3, the faster (τ_1) time is 2.33 ns for the as-grown one, and the contribution is 68.02%. However, the pulse height spectrum shows that the introduction of 2.5 mol % Al will reduce the light yield of the β-Ga_2O_3 crystal.

Keywords: Al-doped β-Ga_2O_3; scintillation; oxygen vacancies

Citation: Tian, R.; Pan, M.; Sai, Q.; Zhang, L.; Qi, H.; Mohamed, H.F. Crucial Role of Oxygen Vacancies in Scintillation and Optical Properties of Undoped and Al-Doped β-Ga_2O_3 Single Crystals. *Crystals* **2022**, *12*, 429. https://doi.org/10.3390/cryst12030429

Academic Editor: László Kovács

Received: 10 February 2022
Accepted: 17 March 2022
Published: 19 March 2022

1. Introduction

The scintillation detection system has the advantages of high detection efficiency and fast time response, and has important applications in high-energy physics experiment, nuclear physics experiment, nuclear medicine imaging and other fields [1]. The scintillation materials play an important role in scintillation detection systems. They can absorb the energy of high-energy particles or rays, convert them into visible light or near-ultraviolet light, and then detect visible or near-ultraviolet light through photomultiplier tubes or CCD and other photodetectors. Therefore, scintillation materials can be used to detect high-energy particles or X-rays and gamma rays. The performance of scintillation materials is closely related to the performance of scintillation detection systems. Excellent scintillation materials should have the characteristics of high light yield, fast scintillation decay time, excellent radiation resistance, matching emission spectrum with the response band of photodetector, and stable physical and chemical properties [2]. Scintillation materials can be divided into organic scintillation materials and inorganic scintillation materials. Inorganic scintillation materials usually have higher effective atomic number, larger densities, and have a strong ability to cut off high-energy particles or high-energy rays. Single crystal inorganic scintillation materials also tend to have higher luminous efficiency. Compared with dielectric scintillators, among single crystal inorganic scintillators, wide band gap semiconductor scintillators have the advantages of ultrafast scintillation decay time and better energy resolution. However, the self-absorption effect of semiconductor scintillation materials limits their wide application in the field of scintillation. For example, the Stokes shift of CuI at room temperature is small, and there is a serious self-absorption effect, which has an adverse effect on the light yield [3].

The β-Ga_2O_3 single crystal is a new type of ultra-wide bandgap(~4.9 eV) semiconductor material, which has important application value in high-power electronic devices and solar-blind ultraviolet detection [4]. In addition, the scintillation properties of β-Ga_2O_3 have attracted extensive research in recent years and other fields, and has attracted extensive research in recent years. The fast scintillation properties of β-Ga_2O_3 single crystals were first reported by Yanagida et al. in 2016, the X-ray excited emission band was around 380 nm with two exponential decay components 8 ns and 977 ns, while the ^{137}Cs 662 keV γ-ray induced light yield was 15,000 ± 1500 ph/MeV [5]. In 2017, Usui et al. reported scintillation features of Ce-doped β-Ga_2O_3, the emission peak was around 420 nm due to the 5d–4f transition of Ce^{3+}, other than 380 nm in undoped β-Ga_2O_3, meanwhile, the decay time became slower [6]. In 2019, Mykhaylyk et al. calculated the theoretical light yield of gallium oxide single crystal, which can reach 40,800 ph/MeV [7]. In 2020, Galazka et al. studied undoped, singly (Ce, Si, Al), doubly (Ce + Si, Ce + Al), and triply (Ce + Si + Al) doped β-Ga_2O_3 crystals, the highest light yield was 7040 ph/MeV for low carrier concentration samples, while the energy resolution was around 10% [8]. All these results show that β-Ga_2O_3 is a promising ultrafast scintillator which needs further research.

For the luminous mechanism, Binet et al. reported [9] that β-Ga_2O_3 has ultraviolet (UV) and blue-band (BB) emissions ascribed to the recombination of self-trapped excitons and donor-acceptor pairs, respectively. UV emission is considered an important factor because of its fast decay time constant is several nanoseconds [10], indicating that it can be used as an ultrafast scintillator in the nuclear radiation detection. Moreover, we cannot deny the main role of intrinsic defects in changing their optical and scintillation properties, especially the oxygen and gallium vacancy defects. Therefore, this work focuses on how to manage the energy band gap to give greater flexibility to design and improve the performance of these devices. In this article, the effects of annealing in different atmospheres (oxygen, nitrogen) and the introduction of Al elements on the scintillation and optical properties of β-Ga_2O_3 single crystals were investigated.

2. Experimental Procedure

Undoped and 2.5 mole% Al-doped β-Ga_2O_3 crystals were prepared using the floating zone method by Quantum Design IRF01-001-00 infrared image furnace, as described in the previous report [11]. The samples used in this work have two types, one is as-grown crystals, and the second is as-annealed in the oxygen and nitrogen at 1400 °C for 20 h, respectively. The optical properties were performed by a PerkinElmer Lambda 750 UV/VIS/NIR Spectrometer (Massachusetts, USA). X-ray excited luminescence (XEL) spectra, photoluminescence (PL) spectrum and decay time profiles were carried by a fluorescence spectrometer (Edinburgh Instrument FLS1000, Edinburgh, UK). The X-ray source with Ag target operating at 50 kV and 15 μA was used as an excitation source. Pulse height spectra was implemented using a ^{137}Cs γ ray source, an ORTEC digiBASE 1024 channel analyzer and a photomultiplier tube (PMT; Hamamatsu R878 with the shaping time of 0.75 μs, Hamamatsu, Japan). All measurements were performed at room temperature.

3. Experimental Results and Discussion

Transmission spectra as a function of incident wavelength (200–1300 nm) for undoped and 2.5 mole% Al-doped β-Ga_2O_3 single crystals as-grown and as-annealed in oxygen and nitrogen are shown in Figure 1. The transmittance of undoped β-Ga_2O_3 samples after annealing in oxygen or nitrogen atmosphere is higher than that of Al-doped β-Ga_2O_3 treated with the same annealing conditions. Under the same annealing conditions (oxygen, nitrogen), the transmittance of undoped β-Ga_2O_3 samples is higher than that of Al-doped β-Ga_2O_3 samples, and the transmittance of undoped gallium oxide samples annealed by oxygen is the highest among all samples. The absorption edge of β-Ga_2O_3 has a slight blue shift with 2.5 mole% Al-doped. Moreover, all transmittances were characterized by downtrends in the IR region [12], except the O_2-annealed of Al-doped β-Ga_2O_3 crystal. The

inset of Figure 1 reveals the optical band gap estimated by a Tauc plot [13], and tabulated in Table 1.

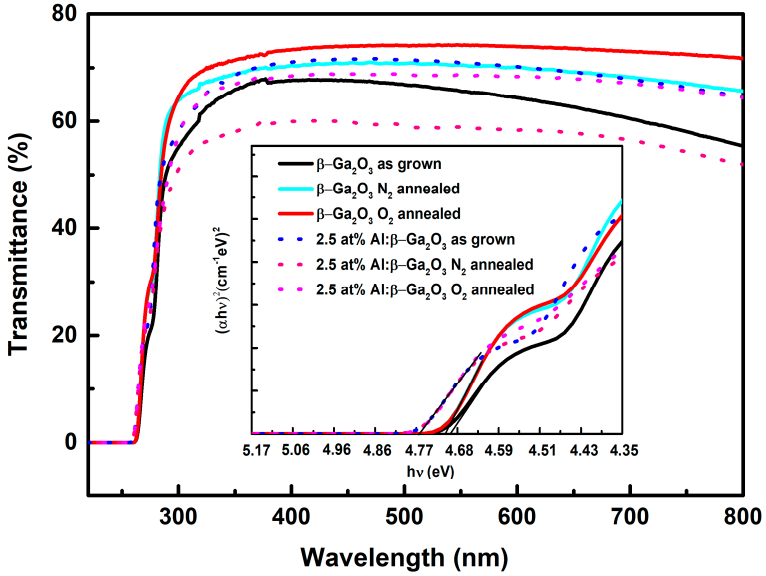

Figure 1. Transmittance of undoped β-Ga_2O_3 and 2.5 mole% Al-doped β-Ga_2O_3 single crystals as-grown and as-annealed process.

Table 1. XEL (X-ray excited luminescence), PL (photoluminescence), energy gap and PL decay time constants of undoped and 2.5 mole% Al-doped β-Ga_2O_3 (Ex. 270 nm, Em. 380 nm).

Sample x	β-Ga_2O_3 as-Grown	β-Ga_2O_3 as-O_2 Annealed	β-Ga_2O_3 as-N_2 Annealed	Al:β-Ga_2O_3 as-Grown	Al:β-Ga_2O_3 as-O_2 Annealed	Al:β-Ga_2O_3 as-N_2 Annealed
X-ray excited luminescence						
XEL-UV(eV), Contr.%	3.62, 31.51	3.61, 36.59	3.64, 28.52	3.69, 33.3	3.678, 19.19	3.68, 27.90
XEL-UV′(eV), Contr.%	3.25, 12.60	3.26, 21.73	3.27, 16.5	3.26, 34	3.27, 29.16	3.30, 28.83
XEL-Blue(eV), Contr.%	3.16, 55.87	3.06, 41.66	3.15, 54.92	2.87, 32.25	2.93, 51.63	3.009, 43.25
Photoluminscence						
PL-UV(eV), Contr.%	3.51, 12.05	3.48, 17.65	3.37, 18.95			
PL-UV′(eV), Contr.%	3.20, 25.82	3.10, 45.35	2.93, 31.50	3.01 44.54	3.02 43.98	3.07 49.24
PL-Blue(eV), Contr.%	2.52, 62.12	2.57, 36.99	2.50, 49.53	2.60 55.46	2.47 56.02	2.72 50.76
Optical transmission						
Eg(eV)	4.69	4.71	4.71	4.76	4.76	4.76

Table 1. *Cont.*

Sample x	β-Ga_2O_3 as-Grown	β-Ga_2O_3 as-O_2 Annealed	β-Ga_2O_3 as-N_2 Annealed	Al:β-Ga_2O_3 as-Grown	Al:β-Ga_2O_3 as-O_2 Annealed	Al:β-Ga_2O_3 as-N_2 Annealed
			PL decay time			
τ_1 (ns),	5.22	6.85	7.72	2.33	3.34	4.26
Contri. %	2.78	0.98	2.54	68.02	62.45	9.31
τ_2 (ns),	54.25,	65.70	55.17	41.58	38.14	41.64
Contri. %	17.61	11.04	27.79	6.35	6.87	20.48
τ_3 (ns),	206.5	271.69	153.7	276.77	220.19	170.81
Contri. %	79.61	87.98	69.66	25.63	30.69	70.22

By comparing the transmittance spectra of undoped β-Ga_2O_3 and Al-doped β-Ga_2O_3 samples, it can be found that the doping of Al element can increase the band gap of β-Ga_2O_3. The band gap increased from 4.7 eV to 4.76 eV with 2.5 mole% Al doping, which is consistent with references [14,15]. These can be interpreted as follows:

Defective chemistry reactions of crystals can be illustrated using the Kröger–Vink notation:

$$\frac{1}{2}O_2 \rightarrow V''_{Ga} + O^x_O + 2\dot{h} \quad \text{Excess Oxygen} \quad (1)$$

$$2GaO + \frac{1}{2}O_2 \rightarrow Ga_2O_3 \quad \text{Oxidation of } Ga^{2+} \text{ ions} \quad (2)$$

$$O_O \rightarrow \frac{1}{2}O_2 + \ddot{V}_O + 2e' \quad \text{Oxygen deficiency} \quad (3)$$

$$Al_2O_3 \overset{Ga_2O_3}{\rightarrow} 2\ddot{Al}_{Ga} + V''_{Ga} + 3O_O \quad \text{Charge equilibrium for Al–doped } \beta - Ga_2O_3 \quad (4)$$

$$(V_O V_{Ga})^X + V^X_o \rightarrow (V_O,\ V_G)' + V'_o + hv \quad \text{Simple blue emission mechanism} \quad (5)$$

In these equations only oxygen and gallium vacancies, as well as a pair of charge (V_O, V_{Ga}) vacancies will be taken into consideration.

Equation (1) elucidates that the O_2-annealing process increases the oxidation of Ga^{2+} ions (GaO_x) to form Ga^{3+} ions (Ga_2O_3, Equation (2)) [16] and Ga vacancies V_{Ga} [17], as well as filling the oxygen vacancies Vo with oxygen and forming O^{2-} [18]. V_{Ga} serves as deep acceptors [19], thereby compensating the unintentionally doped shallow donors. The increase in V_{Ga} leads to a reduction in the free electron concentrations [17] that cause an increase in the band gap. The transmittance of the crystals after oxygen annealing in the near-infrared region also increases due to the increase in the concentration of V_{Ga}.

Regarding the increase in the energy gap due to Al doping, 27Al MAS NMR spectra [20] revealed that the percentage of Al was greater in the octahedral than in the tetrahedral sites due to the lower formation energy. Since the ion radius of Al^{3+} (0.0675 nm) at the octahedral site is smaller than the radius of Ga^{3+} (0.076 nm) at the site, the lattice size will shrink after doping with Al element. Hence, the inter-atomic distance of the ions will decrease and increase the binding force will increase resulting in enhancement of the bandgap.

Besides, as seen in Equation (4), an increase in the concentration of V_{Ga} will lead to an increase in the band gap and a blue shift of the absorption cutoff edge. In the O_2-annealing process, as described above, the V_{Ga} concentration of Al-doped β-Ga_2O_3 increases more than that of undoped β-Ga_2O_3. This agrees with Ma et al., report [21], where they have revealed that the formation energy of O vacancy in the Al-doped β-Ga_2O_3 is larger than which in the undoped β-Ga_2O_3. On the other hand, in the N_2-annealing process, the increment rate of V_O is greater than V_{Ga}, which causes a slight enhancing of the band gap.

Figure 2 shows the X-ray excited luminescence (XEL) spectra of undoped β-Ga_2O_3 and Al-doped β-Ga_2O_3 single crystals as-grown and as-annealed in oxygen and nitrogen at room temperature. The XEL spectra presented mainly consist of two ultraviolet (UV~3.6 eV,

UV′~3.25 eV) and blue-band (BB~3.06 eV) emissions after well-fitted by Gaussian analysis. The luminous intensities of O_2 or N_2 annealed β-Ga_2O_3 crystals are apparently higher than the unannealed one, while it is contrary in Al doped crystals, which is caused by the combined action of self-absorption and luminous efficiency. In undoped β-Ga_2O_3 crystals, the transmission of as-grown and annealed samples is almost the same, while in Al-doped β-Ga_2O_3 crystals, the transmission in the range of luminous wavelength of the as-grown, O_2 annealed and N_2 annealed sample is about 72%, 55%, and 69%, respectively. For undoped β-Ga_2O_3 crystals, the O_2 annealed sample possesses the highest XEL intensity. However, for Al doped crystals, the XEL peak intensity at 345 nm of the as-grown, O_2 annealed and N_2 annealed sample is about 12.2×10^4, 8.5×10^4, and 7.5×10^4, respectively. Thus, we can conclude that O_2 annealing can increase the luminous intensity for undoped β-Ga_2O_3. Besides, by comparing Figure 2a,b, we can see that the as-grown Al-doped β-Ga_2O_3 has a higher XEL spectral intensity than the as-grown undoped β-Ga_2O_3 sample. The introduction of Al element is beneficial to improve the XEL spectrum intensity of the as-grown β-Ga_2O_3.

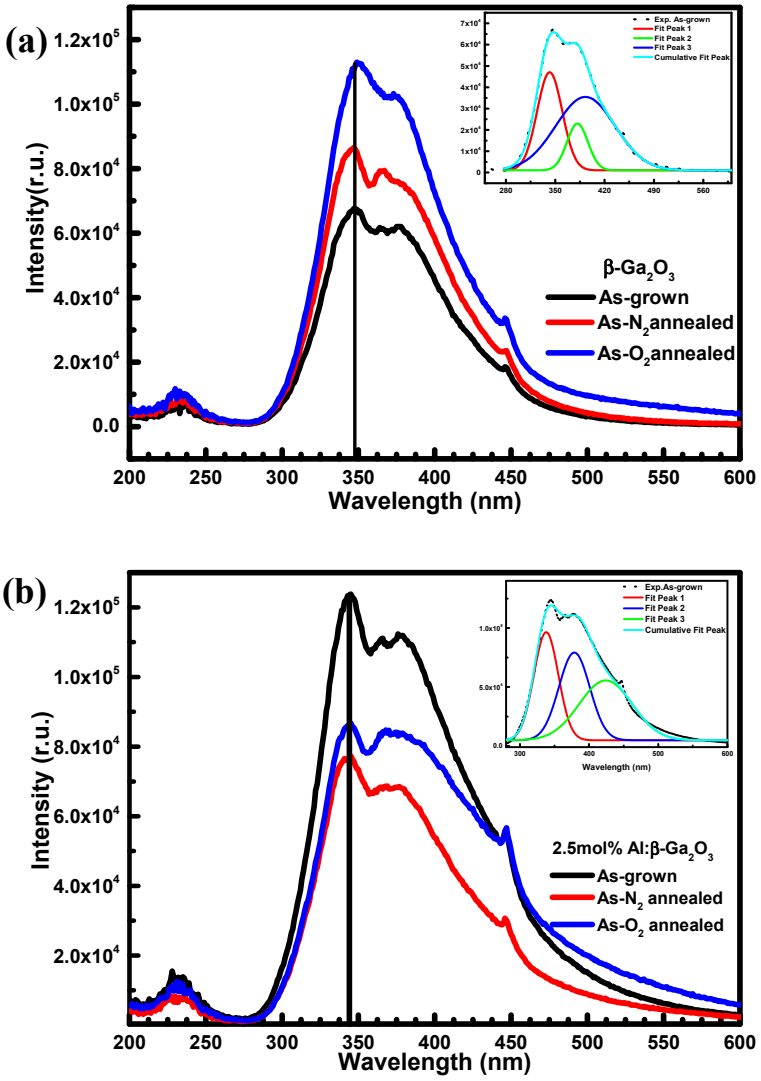

Figure 2. X-ray luminescence spectra of (**a**) pure and (**b**) 2.5 mole% Al-doped β-Ga_2O_3 crystal.

As can be seen from Table 1, for Al-doped β-Ga_2O_3, XEL spectra also consist of two ultraviolet (UV~3.69 eV, UV′~3.3 eV) and blue-band (BB~2.87 eV) emissions after well-fitted by Gaussian analysis. The percentage of (UV and UV′) contribution to total luminescence decrease while BB increases under both annealing processes, besides UV′ and

BB peak positions have a slight shift to higher energy after annealing. Since UV emission is an intrinsic property of crystals, it generally does not depend on specific impurities and appears due to recombination of free electrons and self-trapped hole (STHs) that are confined to $O_{(I)}$ and $O_{(II)}$ sites [22]. On the other hand, BB (BB~3.06 eV) is an extrinsic property that strongly depends on the impurities and heat treatment of crystals and is attributed to the donor-acceptor recombination assign to (V_{Ga} + V_O) defects (with a slight contribution of V_{Ga}) [9].

It can be seen from the above that the luminescence peak positions and intensity of the UV band and the BB bands of the β-Ga_2O_3 single crystal can be controlled by means of Al element doping and oxygen or nitrogen annealing. Therefore, it can be interpreted that as follows:

Intrinsic UV emission increases further with the O_2-annealing process since more carriers in impurity levels can be liberated to conduction and valence bands that are captured again via self-trapped excitons accompanied by a UV photon emission [23,24]. Al doping effect decreases the carrier concentrations that make the electrons in bands are more easily excited to form an exciton resulting in a higher exciton density. Thereby, reducing the excitation energy under the O_2-annealing process leads to a red shift, while in the N_2-annealing process the excitation energy increase leads to a blue shift. According to the Equation (4), extrinsic BB emissions occur by transferring an electron trapped on a donor site (V_O) to a hole created on an acceptor (V_{Ga} or V_O, V_{Ga}) after the acceptor's excitation [9]. For the Al-doped β-Ga_2O_3, the decrease in the luminescence intensity of the blue band after annealing in oxygen atmosphere is caused by the increase in the concentration of V_{Ga} and the decrease in the concentration of V_O [25]. In addition, the increased probability of non-radiative transition recombination of excited carriers is also the reason for the decrease in the luminescence intensity of the blue band.

Figure 3 shows PL spectra of undoped and Al-doped β-Ga_2O_3 single crystals as-grown and annealed in oxygen and nitrogen under an excitation wavelength of 270 nm. After Gaussian fitting, two ultraviolet (UV~3.5 eV, UV′~3.2 eV) and blue-band (BB~2.5 eV) emissions were observed for undoped one, while for Al-doped β-Ga_2O_3 is observed ultraviolet (UV′~3.0 eV) and blue-band (BB~2.5 eV) emissions. This is due to the increase of band gap by Al doping. The excitation energy is 4.59 eV (270 nm), which is lower than the band gap of the undoped β-Ga_2O_3 (4.69 eV~4.71 eV) and the Al-doped β-Ga_2O_3 (4.76 eV). Thus, the intrinsic UV emission disappear in Al doped crystals, and decrease in undoped one.

PL spectra have the same trend as in the XEL spectra. Moreover, the difference between these spectra is that the PL can easily detect defect points more than XEL, besides X-ray generates more free charges that contribute to generating more self-trapped excitons causing the increased appearance of UV emission.

PL decay curve profiles are represented in Figure 4. Decay curves were well fitted with 3-exponential functions for undoped and Al doped β-Ga_2O_3 using the most accurate time-resolved analysis as follows [26];

$$I(t) = a_0 + \sum_{i=1}^{3} a_i \exp\left(\frac{-t}{\tau_i}\right) \quad (6)$$

where a_0 is background signal, a_i and τ_i are intensity and decay time. Besides, the contribution of each decay component can be determined by

$$f_i = \frac{a_i \tau_i}{\sum a_i \tau_i} \quad (7)$$

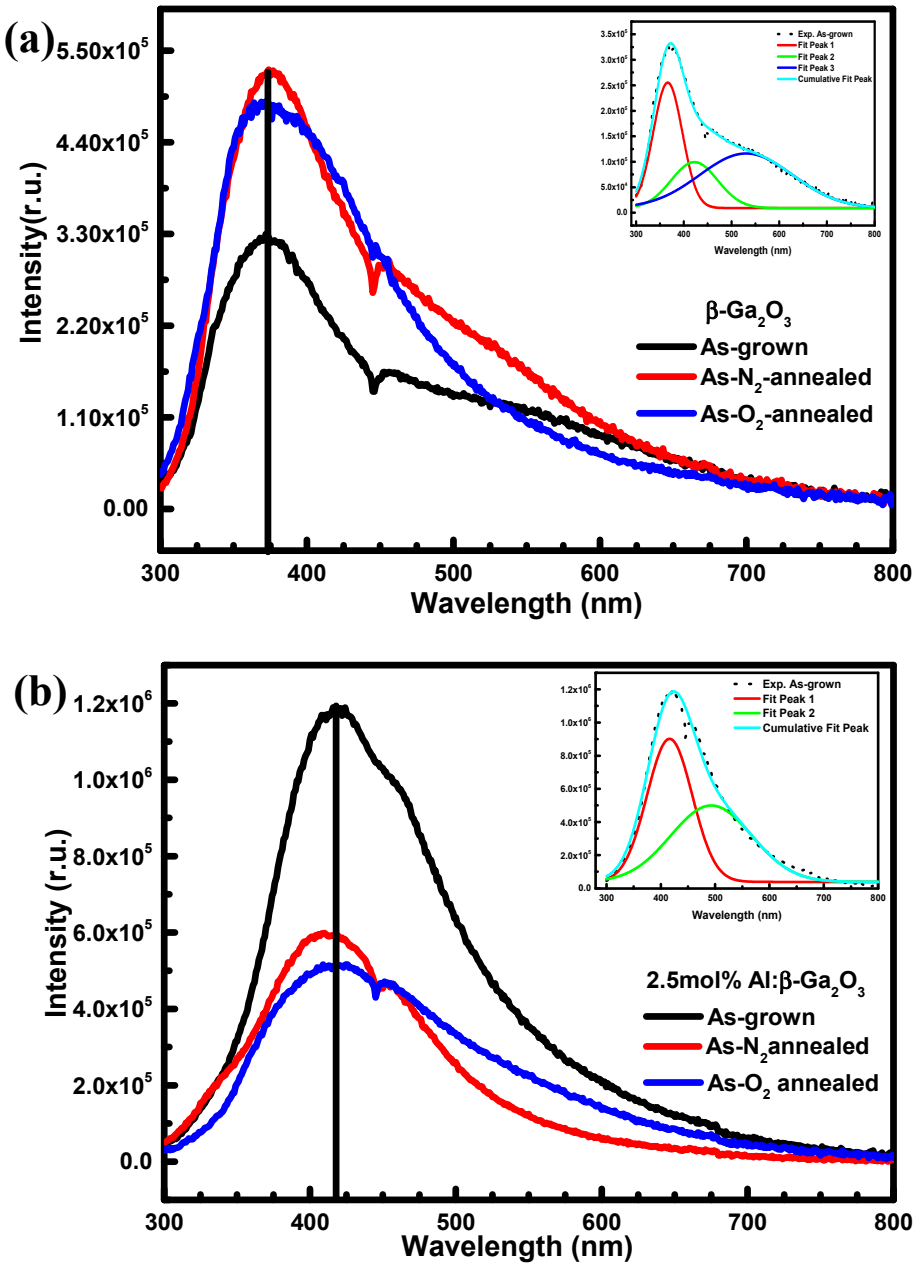

Figure 3. PL emission spectra of (**a**) pure and (**b**) 2.5 mole% Al-doped β-Ga_2O_3 crystal.

The decay time constants of undoped have two components faster (τ_1 and τ_2) and slower (τ_3) with approximate order nanoseconds, and for Al-doped have two faster components (τ_1 and τ_2) and a slower component(τ_3) with approximate values of order nanoseconds and several hundred nanoseconds, respectively. For undoped as-grown β-Ga_2O_3 single crystal, the decay time constants are about 5.22, 54.25, and 206.55 ns, and, also, have similar values reported in the previous work [5]. For the undoped β-Ga_2O_3, the O_2/N_2-annealing will increase the fast component (τ_1), and, also, decrease the proportion of the fast component in the decay time. The increase in the decay time of the undoped β-Ga_2O_3 crystals after annealing is affected by many factors, and the increase in the concentration of V_{Ga} will also lead to an increase in the decay time. For the as-grown Al-doped β-Ga_2O_3, the fast component (τ_1) time is even faster than the undoped β-Ga_2O_3 and the contribution is as large as 68%. In turn, the O_2/N_2-annealing process slightly decreases the fast component.

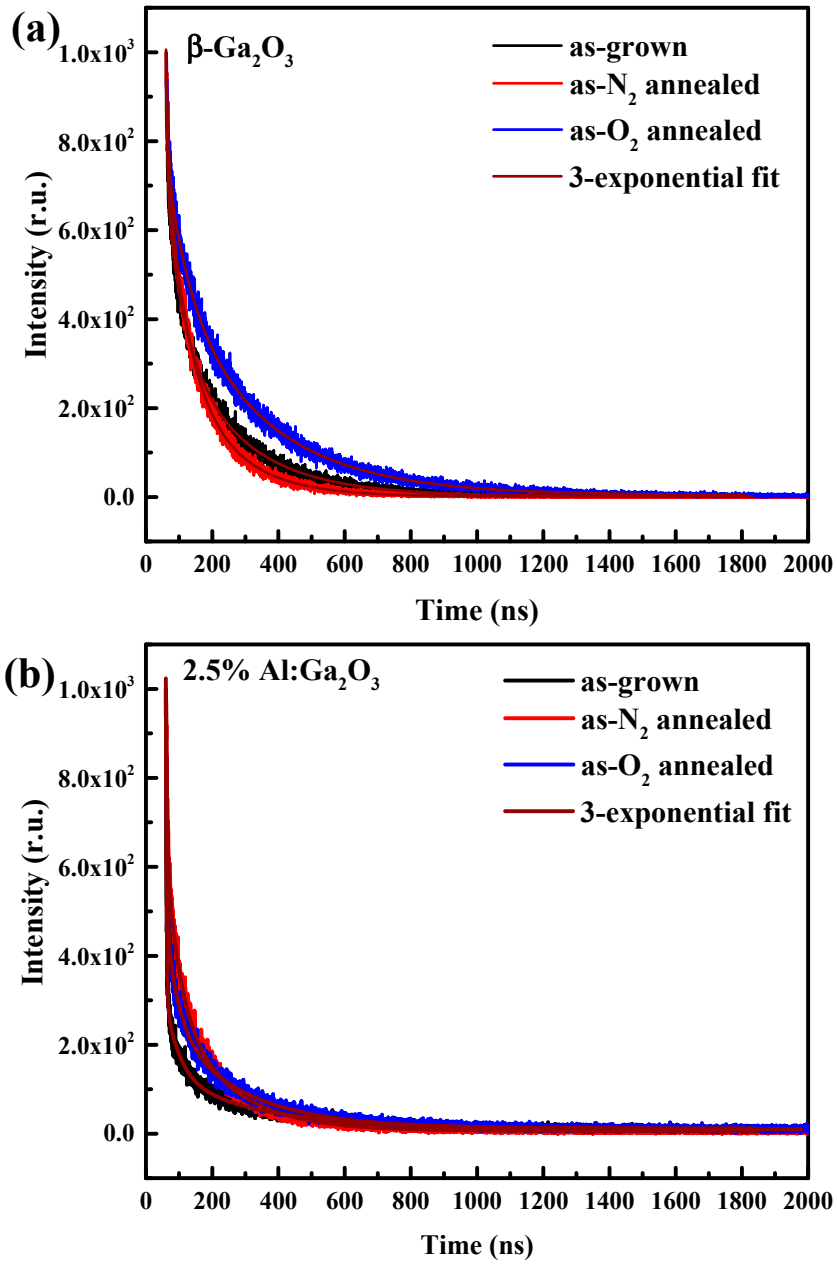

Figure 4. PL decay profiles of (**a**) undoped β-Ga_2O_3 and (**b**) 2.5 mole% Al-doped β-Ga_2O_3 crystal. (Ex. 270 nm, Em. 380 nm).

Pulse height spectra profiles are represented in Figure 5. It can be seen from Figure 5a that the light yield of the undoped β-Ga_2O_3 single crystal after annealing is increased compared with that of the as-grown sample. However, in Figure 5b, the light yield of the annealed Al-doped sample decreased compared with the as-grown sample. This is basically consistent with the trend of XEL and PL spectra. Besides, the undoped β-Ga_2O_3 annealed in the same atmosphere have higher light yields than Al-doped β-Ga_2O_3, which is consistent with the trend reported by Galazka et al. [8] that the introduction of Al element may reduce the light yields of β-Ga_2O_3. The mechanism behind this result needs further study.

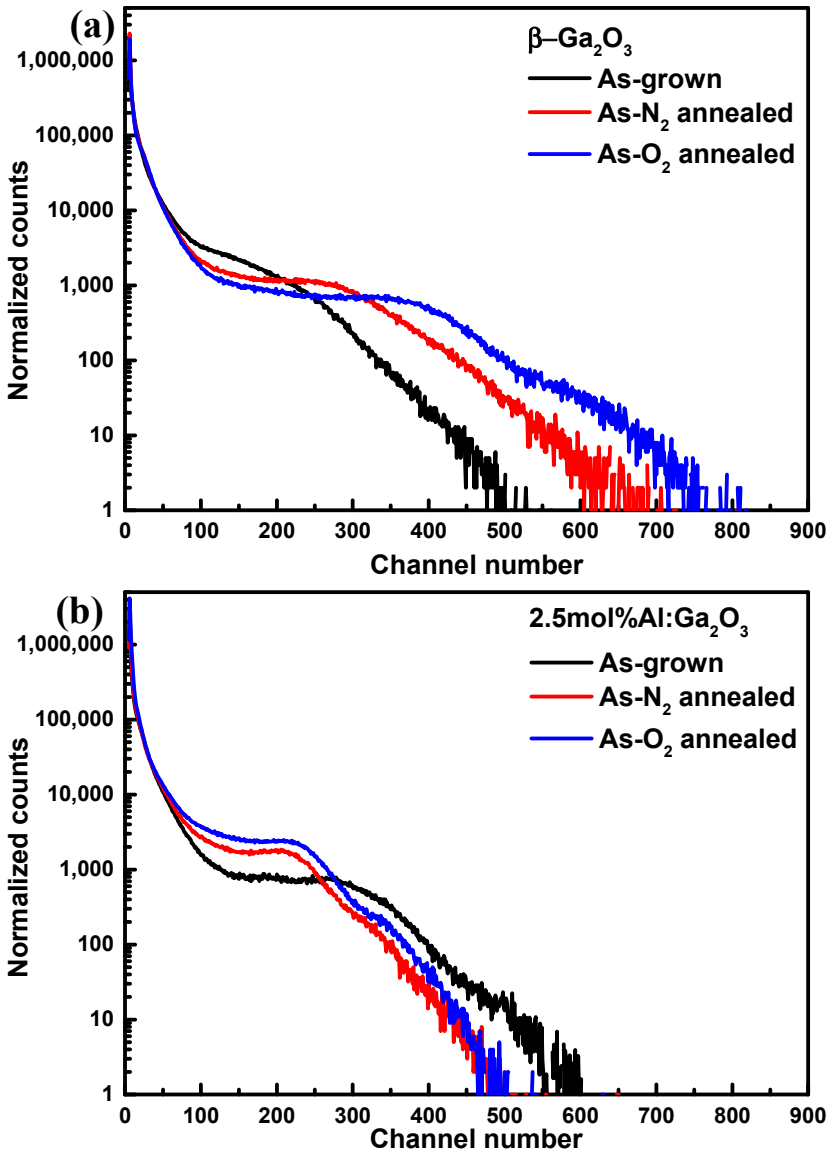

Figure 5. Pulse height spectra profiles of (**a**) undoped β-Ga_2O_3 and (**b**) 2.5 mole% Al-doped β-Ga_2O_3 crystal.

Summary, based on the experimental data of PL, XEL and pulse height spectra techniques, the UV-blue paradigm of undoped β-Ga_2O_3 under the O_2-annealing process is constructed and presented in Figure 6. The O_2-annealing process affects the following:

- Increases Ga^{3+} ions and V_{Ga} acceptors, as well as reduces V_O donors by filling the oxygen vacancies V_O with oxygen and forming O_2^- (process num. 1).
- Increases release of more charge carriers (electron, holes) that are in impurity levels (donors, acceptors) to conduction and valence bands, as they are captured again via self-trapped excitons accompanied by a UV photon emission (process num. 2).
- UV′ and blue emissions occur by transferring an electron trapped on a donor site (V_O) to a hole created on an acceptor (V_{Ga} or V_O, V_{Ga}) after the acceptor's excitation (process num. 3)
- Decrease in the blue luminescence intensity has two reasons, the first is due to an increase in V_{Ga} acceptors and a decrease in V_O donors at the expense of (V_O, V_{Ga}) pairs, and the second is due to the excited carriers in levels have a high probability to non-radiative recombination transfer (process num 4).

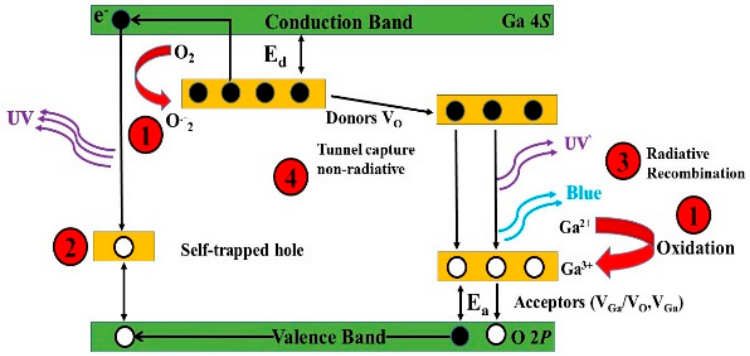

Figure 6. The paradigm of β-Ga_2O_3 during the O_2 annealing process.

4. Conclusions

This paper has explained in more details the role of both oxygen and gallium vacancies in X-ray excited luminescence (XEL) and photoluminescence properties during the oxygen and nitrogen annealing process of the undoped β-Ga_2O_3 and the Al-doped β-Ga_2O_3 crystals, which were grown by floating zone method. According to the transmittance spectrum, an enhancement in the band gap of the β-Ga_2O_3 crystal through the O_2-annealing process or by doping Al element, and in the shape of the shoulder that appears near the absorption edge owing to its anisotropic electronic structure. Luminescence spectra revealed two emission bands in the UV and blue regions are ascribed to the recombination of self-trapped excitons and donor-acceptor pairs, respectively. The total luminescence can be managed by UV and BB emission under Al-doping or annealing process. The fast decay time constants (τ_1) of undoped β-Ga_2O_3 are about 5 ns, and the contribution of the fast decay time is 2.78%. Moreover, for Al-doped β-Ga_2O_3, the fast (τ_1) time is only 2.33 ns, even faster than the undoped one, the contribution of the fast component is higher than 68%, which indicates that Al-doped β-Ga_2O_3 has a great potential as fast crystal scintillator. The pulse height spectrum shows that oxygen annealing is more beneficial to improve the light yield of undoped β-Ga_2O_3, and Al element doping has an adverse effect on the light yield of β-Ga_2O_3.

Author Contributions: Data curation, R.T., L.Z. and H.F.M.; formal analysis, R.T., Q.S. and H.F.M.; writing—original draft, R.T.; conceptualization, M.P.; funding acquisition, M.P. and H.Q.; methodology, M.P., Q.S. and H.F.M.; supervision, M.P.; writing—review & editing, M.P. and H.F.M.; resources, H.Q. All authors have read and agreed to the published version of the manuscript.

Funding: This work was funded by the National Natural Science Foundation of China (Grant No. 52002386, 11535010, 51802327, 51972319) and the Science and Technology Commission of Shang-hai Municipality (No. 19520744400).

Data Availability Statement: Not applicable.

Conflicts of Interest: The authors declare no conflict of interest.

References

1. Dujardin, C.; Auffray, E.; Bourret-Courchesne, E.; Dorenbos, P.; Lecoq, P.; Nikl, M.; Vasil'ev, A.N.; Yoshikawa, A.; Zhu, R.Y. Needs, Trends, and Advances in Inorganic Scintillators. *IEEE Trans. Nucl. Sci.* **2018**, *65*, 1977–1997. [CrossRef]
2. Derenzo, S.E.; Weber, M.J.; Bourret-Courchesne, W.E.; Klintenberg, M.K. The quest for the ideal inorganic scintillator. *Nucl. Instrum. Methods Phys. Res. Sect. A-Accel. Spectrom. Dect. Assoc. Equip.* **2003**, *505*, 111–117. [CrossRef]
3. Yue, S.Q.; Gu, M.; Liu, X.L.; Li, F.R.; Liu, S.Y.; Zhang, X.; Zhang, J.N.; Liu, B.; Huang, S.M.; Ni, C. Optimization of crystal growth and properties of gamma-CuI ultrafast scintillator by the addition of LiI. *Mater. Res. Bull.* **2018**, *106*, 228–233. [CrossRef]
4. Pearton, S.J.; Yang, J.C.; Cary, P.H.; Ren, F.; Kim, J.; Tadjer, M.J.; Mastro, M.A. A review of Ga_2O_3 materials, processing, and devices. *Appl. Phys. Rev.* **2018**, *5*, 56. [CrossRef]
5. Yanagida, T.; Okada, G.; Kato, T.; Nakauchi, D.; Yanagida, S. Fast and high light yield scintillation in the Ga_2O_3 semiconductor material. *Appl. Phys. Express* **2016**, *9*, 4. [CrossRef]

6. Usui, Y.; Oya, T.; Okada, G.; Kawaguchi, N.; Yanagida, T. Ce-doped Ga_2O_3 single crystalline semiconductor showing scintillation features. *Optik* **2017**, *143*, 150–157. [CrossRef]
7. Mykhaylyk, V.B.; Kraus, H.; Kapustianyk, V.; Rudko, M. Low temperature scintillation properties of Ga_2O_3. *Appl. Phys. Lett.* **2019**, *115*, 5. [CrossRef]
8. Galazka, Z.; Schewski, R.; Irmscher, K.; Drozdowski, W.; Witkowski, M.E.; Makowski, M.; Wojtowicz, A.J.; Hanke, I.M.; Pietsch, M.; Schulz, T.; et al. Bulk beta-Ga_2O_3 single crystals doped with Ce, Ce plus Si, Ce plus Al, and Ce plus Al plus Si for detection of nuclear radiation. *J. Alloys Compd.* **2020**, *818*, 7. [CrossRef]
9. Binet, L.; Gourier, D. Origin of the blue luminescence of beta-Ga_2O_3. *J. Phys. Chem. Solids* **1998**, *59*, 1241–1249. [CrossRef]
10. He, N.T.; Tang, H.L.; Liu, B.; Zhu, Z.C.; Li, Q.; Guo, C.; Gu, M.; Xu, J.; Liu, J.L.; Xu, M.X.; et al. Ultra-fast scintillation properties of beta-Ga_2O_3 single crystals grown by Floating Zone method. *Nucl. Instrum. Methods Phys. Res. Sect. A-Accel. Spectrom. Dect. Assoc. Equip.* **2018**, *888*, 9–12. [CrossRef]
11. Cui, H.Y.; Mohamed, H.F.; Xia, C.T.; Sai, Q.L.; Zhou, W.; Qi, H.J.; Zhao, J.T.; Si, J.L.; Ji, X.L. Tuning electrical conductivity of beta-Ga_2O_3 single crystals by Ta doping. *J. Alloys Compd.* **2019**, *788*, 925–928. [CrossRef]
12. Ueda, N.; Hosono, H.; Waseda, R.; Kawazoe, H. Synthesis and control of conductivity of ultraviolet transmitting beta-Ga_2O_3 single crystals. *Appl. Phys. Lett.* **1997**, *70*, 3561–3563. [CrossRef]
13. Tauc, J. *Amorphous and Liquid Semiconductors*; Springer: Boston, MA, USA, 1974; p. 159.
14. Galazka, Z.; Ganschow, S.; Fiedler, A.; Bertram, R.; Klimm, D.; Irmscher, K.; Schewski, R.; Pietsch, M.; Albrecht, M.; Bickermann, M. Doping of Czochralski-grown bulk beta-Ga_2O_3 single crystals with Cr, Ce and Al. *J. Cryst. Growth* **2018**, *486*, 82–90. [CrossRef]
15. Bhaumik, I.; Soharab, M.; Bhatt, R.; Saxena, A.; Sah, S.; Karnal, A.K. Influence of Al content on the optical band-gap enhancement and lattice structure of $(Ga_{1-x}Al_x)_{(2)}O_3$ single crystal. *Opt. Mater.* **2020**, *109*, 6. [CrossRef]
16. Feng, Z.Q.; Huang, L.; Feng, Q.; Li, X.; Zhang, H.; Tang, W.H.; Zhang, J.C.; Hao, Y. Influence of annealing atmosphere on the performance of a beta-Ga_2O_3 thin film and photodetector. *Opt. Mater. Express* **2018**, *8*, 2229–2237. [CrossRef]
17. Tang, H.L.; He, N.T.; Zhu, Z.C.; Gu, M.; Liu, B.; Xu, J.; Xu, M.X.; Chen, L.; Liu, J.L.; Ouyang, X.P. Temperature-dependence of X-ray excited luminescence of beta-Ga_2O_3 single crystals. *Appl. Phys. Lett.* **2019**, *115*, 5. [CrossRef]
18. Feng, H.; Ding, D.Z.; Li, H.Y.; Lu, S.; Pan, S.K.; Chen, X.F.; Ren, G.H. Annealing effects on Czochralski grown $Lu_2Si_2O_7$: Ce^{3+} crystals under different atmospheres. *J. Appl. Phys.* **2008**, *103*, 7. [CrossRef]
19. Gao, H.T.; Muralidharan, S.; Pronin, N.; Karim, M.R.; White, S.M.; Asel, T.; Foster, G.; Krishnamoorthy, S.; Rajan, S.; Cao, L.R.; et al. Optical signatures of deep level defects in Ga_2O_3. *Appl. Phys. Lett.* **2018**, *112*, 5. [CrossRef]
20. Kaun, S.W.; Wu, F.; Speck, J.S. beta-$(Al_xGa_{1-x})(2)O_3/Ga_2O_3$ (010) heterostructures grown on beta-Ga_2O_3 (010) substrates by plasma-assisted molecular beam epitaxy. *J. Vac. Sci. Technol. A* **2015**, *33*, 9. [CrossRef]
21. Ma, X.F.; Zhang, Y.M.; Dong, L.P.; Jia, R.X. First-principles calculations of electronic and optical properties of aluminum-doped beta-Ga_2O_3 with intrinsic defects. *Results Phys.* **2017**, *7*, 1582–1589. [CrossRef]
22. Onuma, T.; Nakata, Y.; Sasaki, K.; Masui, T.; Yamaguchi, T.; Honda, T.; Kuramata, A.; Yamakoshi, S.; Higashiwaki, M. Modeling and interpretation of UV and blue luminescence intensity in beta-Ga_2O_3 by silicon and nitrogen doping. *J. Appl. Phys.* **2018**, *124*, 6. [CrossRef]
23. Varley, J.B.; Janotti, A.; Franchini, C.; Van de Walle, C.G. Role of self-trapping in luminescence and p-type conductivity of wide-band-gap oxides. *Phys. Rev. B* **2012**, *85*, 4. [CrossRef]
24. Shi, Q.; Wang, Q.R.; Zhang, D.; Wang, Q.L.; Li, S.H.; Wang, W.J.; Fan, Q.L.; Zhang, J.Y. Structural, optical and photoluminescence properties of Ga_2O_3 thin films deposited by vacuum thermal evaporation. *J. Lumines.* **2019**, *206*, 53–58. [CrossRef]
25. Vasiltsiv, V.I.; Zakharko, Y.M.; Rym, Y.I. On the nature of blue and green luminescence bands of BETA-Ga_2O_3. *Ukr. Fiz. Zhurnal* **1988**, *33*, 1320–1324.
26. Ahmadi, E.; Koksaldi, O.S.; Zheng, X.; Mates, T.; Oshima, Y.; Mishra, U.K.; Speck, J.S. Demonstration of beta-$(Al_xGa_{1-x})_{(2)}O_3$/beta-Ga_2O_3 modulation doped field-effect transistors with Ge as dopant grown via plasma-assisted molecular beam epitaxy. *Appl. Phys. Express* **2017**, *10*, 4. [CrossRef]